1.D.1 *Nuclear Physics* A289 (1977) 346–364;

AN ASYMPTOTIC FORM OF THE SMOOTH PART OF THE TOTAL SINGLE-PARTICLE ENERGY

ADAM SOBICZEWSKI
The Niels Bohr Institute, Copenhagen, Denmark
and
Institute for Nuclear Research, Hoza 69, 00-681 Warszawa, Poland †

ANNA GYURKOVICH
Institute for Nuclear Research, Hoza 69, 00-681 Warszawa, Poland

and

MATTHIAS BRACK ††
The Niels Bohr Institute, Copenhagen, Denmark

Received 16 May 1977

Abstract: A method of separating the smooth part from the sum of the single-particle energies is discussed. The method consists of an expansion of this smooth part in the asymptotic series, i.e. in a series in powers of $A^{-1/3}$. The series is studied numerically in the case of a finite (Woods-Saxon) potential with realistic depth and surface thickness parameters. The Strutinsky smooth part of the energy is also extensively studied and compared with the asymptotic one.

1. Introduction

The idea of the calculation of the shell correction to the nuclear mass as a difference between the sum of the single-particle energies, obtained in a realistic potential, and its smooth part [1]), resulted in a significant improvement in nuclear masses, as compared with those of the liquid drop. The most practical and effective method of extraction of this smooth part was proposed by Strutinsky [2]). The method has been widely applied to the calculations of the masses, shapes and fission barriers of nuclei (cf. e.g. refs. [3–5])). Various aspects and especially the problem of accuracy of the method were discussed in a number of papers (e.g. refs. [3–8])). One of these aspects is the effect of unbound states [5, 9]) which should be added when applying the method to a finite-depth potential. The effect introduces some inaccuracy in the smooth part of the energy, especially in the case of lighter nuclei for which the separation energy is comparable with the smearing interval, the latter being of the order of the distance between the major shells.

† Permanent address.
†† Present address: Institut Laue-Langevin, Grenoble, France.

There have also been proposed some other methods for extracting the smooth part of the energy. One of them, suggested recently [10]), is the method of averaging over nucleon number, instead of over energy. This method does not need any unbound levels. In fact, it presents a general method of extracting the smooth part from any fluctuating quantity. Both averaging over the nucleon number and over the energy are particular cases of it.

Other methods are those of the semiclassical expansion [11-16]). They allow one to separate the smooth part of the energy in a well-defined way, also for finite-depth potentials including spin-orbit interaction. For infinite potentials, the equivalence of the semiclassical and the Strutinsky method has been established [15]).

In the present paper, we discuss the method which consists of an expansion of the smooth part of the energy in the asymptotic series, i.e. in a series in powers of $A^{-\frac{1}{3}}$. Such an expansion has been used for a long time [17-21]) for the nuclear binding energy and originated from the liquid-drop formula. The investigations of refs. [17-21]) aimed at the theoretical reproduction of the empirical surface term in this formula. Recently, the liquid-drop formula has been extended [22]) to the next power, i.e. $A^{\frac{1}{3}}$, term (droplet model).

The asymptotic expansion was applied to the sum of the single-particle energies* in refs. [23,24]), where the cases of the infinitely deep orthohombic box [23]) and triaxial harmonic oscillator [24]) potentials were investigated.

The purpose of the present paper is to study the asymptotic expansion in the case of a finite potential. The expansion defines the smooth part of the energy and thus also the shell correction uniquely, making no use of unbound levels. In the numerical calculations, the spherical Woods-Saxon potential is considered. To simplify the study, no spin-orbit and no Coulomb interactions are taken into account. The first few coefficients of the asymptotic series are obtained. The smooth part of the energy calculated in this case by the Strutinsky method is also discussed.

In sect. 2, we describe the asymptotic expansion of the smooth energy, and, in sect. 3, we present the numerical calculations and the results. Results obtained by the Strutinsky method are given in sect. 4. Sect. 5 presents the discussion and sect. 6 gives the conclusions.

2. Method of the asymptotic expansion

Let us assume a large system with a well-defined size L. This requires a small surface diffuseness t with respect to L (thin-surface, leptodermous system). Let us also assume a smooth dependence of the parameters of the corresponding potential on the size L. Then, the smooth part $\tilde{U}$ of the single-particle energy U may be represented as a series in powers of $1/L$ (or, better, t/L):

$$\tilde{U} = \bar{\varepsilon}_{\mathrm{vol}} L^3 + \bar{\varepsilon}_{\mathrm{sur}} L^2 + \bar{\varepsilon}_{\mathrm{cur}} L + \bar{\varepsilon}_0 + \ldots . \tag{2.1}$$

Relating the size L to the mass number A of the system in the way appropriate for

saturating systems,

$$L = rA^{\frac{1}{3}} + b, \tag{2.2}$$

we can expand $\bar{U}$ in powers of $A^{-\frac{1}{3}}$:

$$\bar{U} = \varepsilon_{\text{vol}} A + \varepsilon_{\text{sur}} A^{\frac{2}{3}} + \varepsilon_{\text{cur}} A^{\frac{1}{3}} + \varepsilon_0 + \ldots . \tag{2.3}$$

For any potential, once the relation (2.2) between its size L and the number of particles A is established, the dependence of the single-particle energy U on A is determined. This determines uniquely the coefficients of the series (2.3), with the only exception of the potentials for which the amplitude of the oscillating part of the energy (the shell correction δU) has the same asymptotic dependence on A as one of the terms in the series (2.3). Examples of such potentials are the three-dimensional harmonic oscillator ($\delta U \sim A^{\frac{1}{3}}$) and the infinitely deep cubic box ($\delta U \sim A^0$) (cf. refs. [24, 27]). In such cases an additional condition (e.g. a disappearance of δU at high temperature) is needed for a unique determination of the corresponding coefficient in the series (2.3).

For potentials with simple analytic spectra of the eigenvalues, the series may be found relatively easily. For example, for a spherical harmonic oscillator, only terms with odd powers of $A^{\frac{1}{3}}$ appear. The first few terms of the series are

$$\bar{U} = \tfrac{1}{2}\hbar\omega(\tfrac{3}{2}A)^{\frac{2}{3}}\left\{(\tfrac{3}{2}A) + \tfrac{1}{2}(\tfrac{3}{2}A)^{\frac{1}{3}} + \tfrac{1}{8}(\tfrac{3}{2}A)^{-\frac{1}{3}} + \frac{1}{6\cdot 4^2}(\tfrac{3}{2}A)^{-3/3} - \frac{1}{3\cdot 4^4}(\tfrac{3}{2}A)^{-5/3} + \frac{2}{9\cdot 4^6}(\tfrac{3}{2}A)^{-9/3} - \frac{2}{9\cdot 4^7}(\tfrac{3}{2}A)^{-11/3} + \ldots\right\}, \tag{2.4}$$

where $\hbar\omega$ is the energy spacing between the shells.

Here isospin (as well as spin) degeneracy is assumed. Otherwise we should put $\mathcal{N} = \frac{1}{2}A$ for the number of particles of the same kind and divide the energy by two.

The coefficients of the series (2.4) can be found directly [24]) by expressing both $\bar{U}$ and A in terms of the number N_0 of the last occupied shell and determining $\bar{U}(A)$ by elimination of N_0. The smooth energy $\bar{U}$ is defined in this case as that part of U which is independent of the occupation factor of the last shell. They also can be found, even more conveniently, by using [24]) the smooth part of the level density obtained by a corresponding expansion of the Laplace transform of the exact density [14]).

We can see that the series (2.4) is converging very fastly. For example, taking only the two first terms, we get $\bar{U}$ with an accuracy of about 0.5 MeV (with $\hbar\omega = 41A^{-\frac{1}{3}}$ MeV) for a nucleus with mass number $A \approx 144$.

In a general case, we know only the first (volume) term of the series (2.3). It is the Fermi-gas term. The next ("surface") term can be given analytically for a relatively general potential [25, 26]). Namely, for a potential with an arbitrary radial dependence with the only restriction that it is uniform in its interior region of a large size and that the thickness of its surface region does not depend on this size. No spin-orbit and

no Coulomb interactions are assumed. The formula for ε_{sur} is then [26])

$$\varepsilon_{sur} = \frac{3}{5}\frac{\hbar^2 k_F^2}{2M}\left\{-2\frac{b}{r} + \frac{15}{r k_F^5}\int_0^{k_F} k(k_F^2 - k^2)[\tfrac{1}{4}\pi - \delta(k)]\mathrm{d}k\right\}, \tag{2.5}$$

where k_F is the Fermi momentum, M is the mass of a nucleon, r and b are defined by eq. (2.2), and $\delta(k)$ is the phase shift of the wave function of a nucleon with the momentum k, due to the presence of the surface.

The subsequent, higher order, terms have to be found numerically for finite-depth potentials.

As mentioned in the introduction, we aim at a study of the series (2.3) for the Woods-Saxon potential. No spin-orbit and no Coulomb interactions are assumed. The coefficient ε_{sur} is found from the formula (2.5) and the coefficients ε_{cur} and ε_0 are calculated numerically.

3. Results of the calculations

We start with the presentation of the results for the sum of the single-particle levels $\sum_\nu e_\nu$. More precisely, we will be first concerned with the quantity

$$F(A) \equiv \{\sum_\nu e_\nu - \varepsilon_{vol}A - \varepsilon_{sur}A^{\frac{2}{3}}\}A^{-\frac{1}{3}}, \tag{3.1}$$

which, according to eq. (2.3), is needed for the evaluation of the coefficients ε_{cur} and ε_0. The summation in eq. (3.1) runs over all occupied levels, from the lowest one up to the Fermi level.

The quantity $F(A)$ is presented in fig. 1. The parameters of the potential are the following. The radius R, measured to the half-depth point, is

$$R = 1.27A^{\frac{1}{3}} \text{ fm}. \tag{3.2}$$

Thus, we choose $b = 0$ in relation (2.2) (with the size L being identical with R). The depth is $V_0 = -44$ MeV and the diffuseness is $a = 0.67$ fm.

The volume coefficient ε_{vol} obtained from the Fermi-gas model is in this case $\varepsilon_{vol} = -26.11$ MeV and the surface coefficient ε_{sur} calculated by the formula (2.5) is $\varepsilon_{sur} = 37.40$ MeV.

The shell structure of $F(A)$, equivalent to the shell structure of $\sum_\nu e_\nu$, is clearly seen. It is visible how $F(A)$ varies with a filling of the single-particle levels, each of which is $4(2l+1)$ times degenerate, where l is the orbital angular momentum. Strong shells at (no spin-orbit coupling!) $A = 40$, 80, 140, 184, 276, 396 and 548 are observed.

Fig. 2 illustrates directly the structure of the single-particle spectra for a number of nuclei, of which some are magic while the others have the last shell about half-filled. The Fermi level of each spectrum is denoted by a wavy line and its quantum numbers, n_l, are put in parentheses. It is seen that for the lightest nuclei only one, two or three levels above the Fermi level are bound.

Fig. 3 shows $F(A)$ plotted as a function of $A^{-\frac{1}{3}}$ and not A as given in fig. 1. The

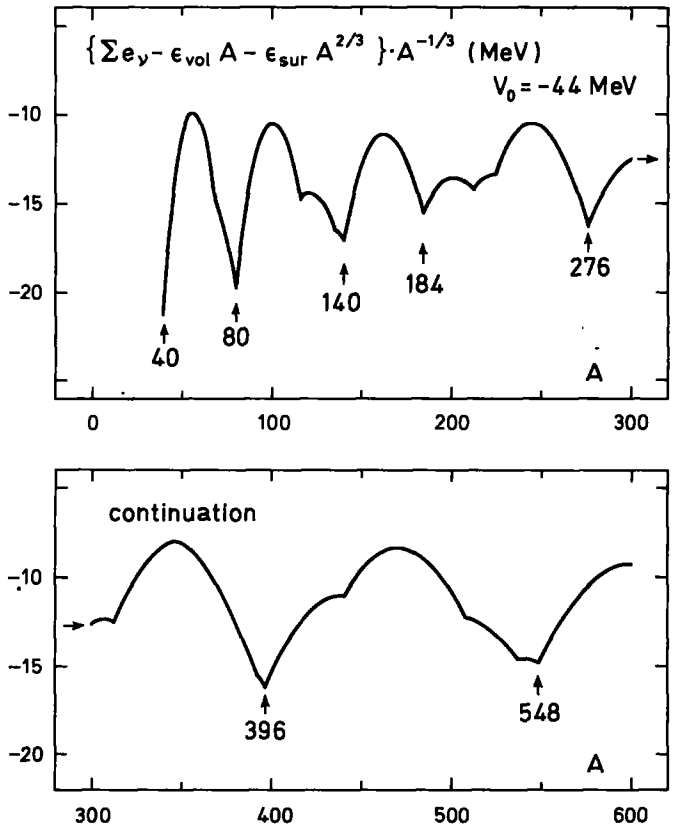

Fig. 1. Dependence of the difference between the sum of the single-particle energies $\sum_\nu e_\nu$ and the volume and surface terms, divided by $A^{1/3}$, on the mass number A. The mass numbers of magic nuclei are shown.

function $F(A)$ is given here in the region of $A^{-\frac{1}{3}}$ from $A^{-\frac{1}{3}} \approx 0.031$ to $A^{-\frac{1}{3}} \approx 0.29$ which corresponds to A from $A = 40$ to $A \approx 30000$. As, starting from about $A \approx 1500$, the plot of $F(A)$ becomes unreadable as function of $A^{-\frac{1}{3}}$, we present only few separate points to give an idea of the behaviour of $F(A)$ for such large mass numbers.

Fig. 3 allows one to get directly the coefficients ε_{cur} and ε_0, being now the ordinate at $A^{-\frac{1}{3}} = 0$ ($A = \infty$) and the slope, respectively, of the straight line drawn as an average of the oscillating quantity $F(A)$. The coefficients much depend, however, on how we draw the straight line. If we put it through around one-third of the amplitudes of the fluctuations of $F(A)$ (considering that the upper $\frac{1}{3}$ will be flattened by the deformation energy, if we allow the deformation degree of freedom), we get $\varepsilon_{cur} \approx -8.2$ MeV and $\varepsilon_0 \approx -33.7$ MeV. This is just the straight line shown in the figure. If we put the line through around one-half of the fluctuation amplitudes, we get $\varepsilon_{cur} \approx -7.0$ MeV and $\varepsilon_0 \approx -35.0$ MeV.

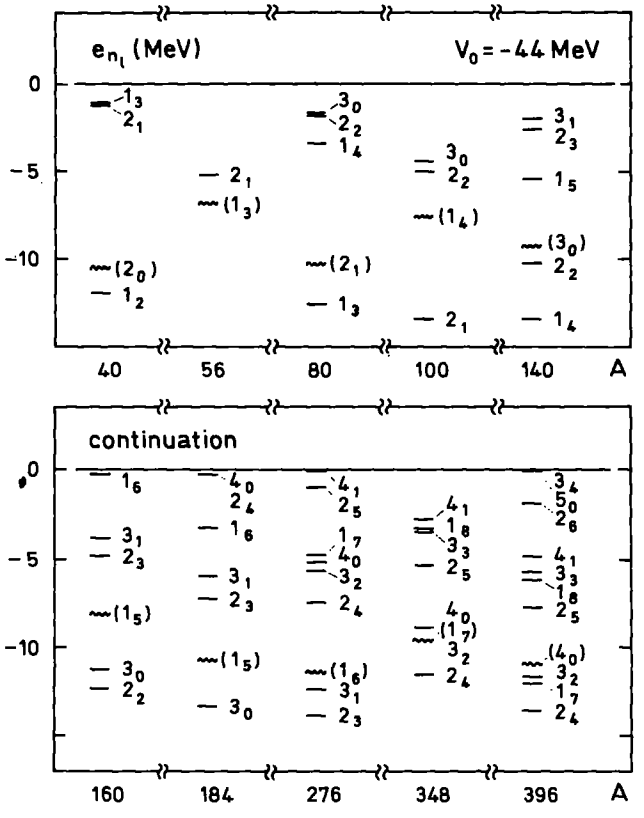

Fig. 2. Single-particle spectra of some magic and some non-magic nuclei. The Fermi levels are shown by wavy lines and their quantum numbers n_l are put into brackets.

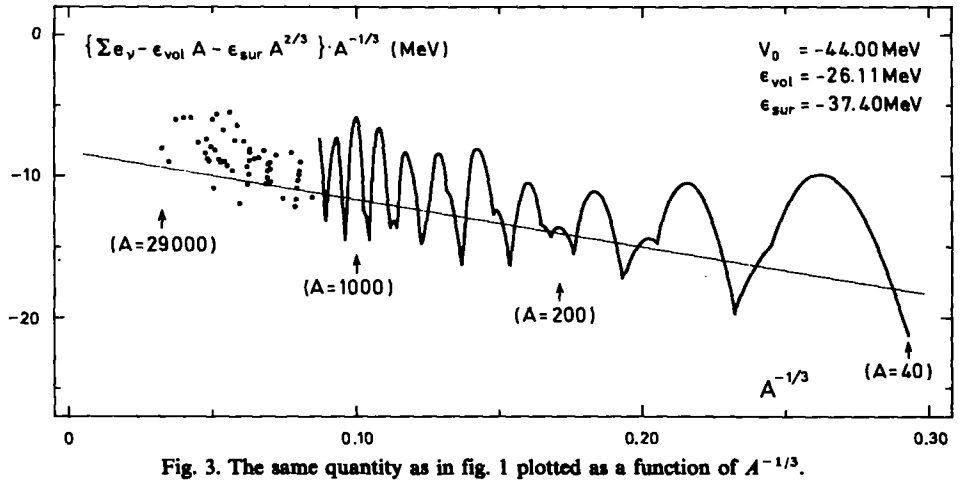

Fig. 3. The same quantity as in fig. 1 plotted as a function of $A^{-1/3}$.

We could also find the coefficients ε_{cur} and ε_0 by a least-square fit of the straight line to $F(A)$. However, as $F(A)$ is a strongly fluctuating quantity, the result of the fit depends quite strongly on the choice of the points.

The parameters of the single-particle potential used above result in separation energies which are about right (i.e. about the experimental values) for light nuclei, but which are too large for heavy nuclei. As can be seen directly from fig. 2, the separation energies obtained for large and medium nuclei ($A < 150$) are around 7–10 MeV, while for heavy nuclei ($A \gtrsim 150$) they are around 8–11 MeV.

It is reasonable then to perform the calculations also for a shallower potential. We choose for that the potential with the depth $V_0 = -38$ MeV, keeping the previous values $R = 1.27\,A^{\frac{1}{3}}$ fm and $a = 0.67$ fm for the radius and the diffuseness unchanged. The separation energies are then around 3–6 MeV for light nuclei, i.e. too small, and around 4–7 MeV for heavy nuclei, i.e. about right. (In this way, we now have a set of two potentials, each of which gives the separation energy about right in their respective regions of nuclei, light or heavy.)

As we decrease only the depth of the potential, the structure of the spectra remains the same in the case of $V_0 = -38$ MeV as was in the case of $V_0 = -44$ MeV. Only the spacings between the levels are smaller, resulting in slightly smaller fluctuations of the function $F(A)$ and thus also in smaller shell corrections. The plot of $F(A)$ for $V_0 = -38$ MeV as a function of $A^{-\frac{1}{3}}$ looks very similar to that of fig. 3, so we do not present it here. The straight line put through around one-third of the amplitudes of the fluctuations gives in this case $\varepsilon_{cur} \approx -16.6$ MeV and $\varepsilon_0 \approx -22.0$ MeV.

The determination of ε_{cur} and ε_0 presented up to now suffers from two deficiencies. One is that it is based mainly on the part of the graph of $F(A)$ corresponding to not very large A (up to about $A = 1500$) and thus ε_{cur} and ε_0 may contain a large contribution from the higher order terms. To avoid this, we should go to much larger A, where the higher terms are negligible. The second disadvantage is the large fluctuation of $F(A)$, being the fluctuation of the shell correction δU damped by the factor $A^{-\frac{1}{3}}$. This large fluctuation of $F(A)$ results in a large uncertainty in the coefficients ε_{cur} and ε_0, and we could not avoid this, even going to the very large A still practical for computation. It is because the amplitude of the shell correction δU for the spherical Woods-Saxon potential is expected [24, 27]) to behave as $A^{1/6}$. Thus, the amplitude of the fluctuation of $F(A)$ is expected to decrease very slowly with A, as $A^{-1/6}$, which agrees roughly with what we see in fig. 3.

We can avoid the second deficiency by smearing out the shell correction. This can be done, e.g., by the Strutinsky method [2]). For a very large A, this method leads to a well defined smooth part of the energy. It is because for a large A, due to the large density of energy levels, there are so many bound levels above the Fermi energy that the unbound levels have no influence on the smooth energy $\tilde{U}$. This will be explicitely illustrated in sect. 4. In other words, a finite-depth potential of a large spatial size behaves effectively as an infinitely deep potential and leads to a well defined smooth part $\tilde{U}$ when the smearing of the levels is applied. There is no

inconsistency then in using the following procedure: We apply the Strutinsky energy smearing for very heavy nuclei to determine the coefficients of the asymptotic series (2.3), which then can be used for the calculation of the smooth energy $\tilde{U}_{as}$ for any (and thus also light) nuclei. Being independent of the unbound levels, $\tilde{U}_{as}$ could be used next, for light nuclei, as a test for the Strutinsky energy $\tilde{U}_{Str}$, which depends on these levels for such nuclei.

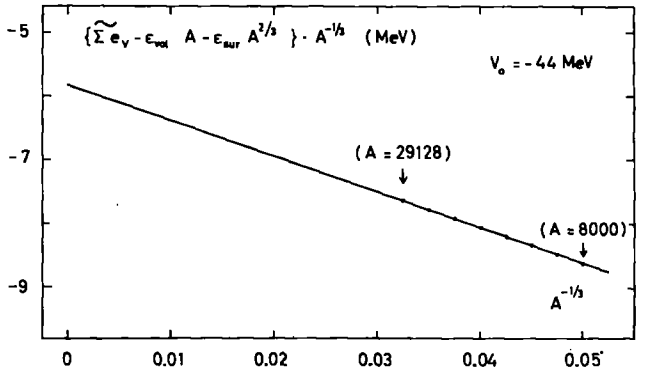

Fig. 4. The same quantity as in fig. 3 after energy smearing of the single-particle levels.

Fig. 4 presents the results for the quantity $\tilde{F}(A)$, eq. (3.1), in which the energies e_ν in the sum $\sum_\nu e_\nu$ are smeared by the Strutinsky method. The results are obtained for eight mass numbers extended from $A = 8000$ to $A = 29128$. We can see that it is not possible to notice any deviation of the points from the straight line, in the scale of the figure. The coefficients ε_{cur} and ε_0 obtained from the line are $\varepsilon_{cur} = -5.84$ MeV and $\varepsilon_0 = -55.9$ MeV. We estimate that in this way, with A going up to around 30000, we determine ε_{cur} with an accuracy of about ± 0.03 MeV and ε_0 with about ± 1.0 MeV.

The same procedure applied to the case of the shallower potential, $V_0 = -38$ MeV, leads to the coefficients $\varepsilon_{cur} = -14.91$ MeV and $\varepsilon_0 = -44.2$ MeV. Here, we go to $A = 37036$ in the calculations. We estimate that an accuracy of about ± 0.03 MeV and ± 1.0 MeV for ε_{cur} and ε_0, respectively, is obtained, the same as in the case of $V_0 = -44$ MeV.

Analyzing the deviation of $\tilde{F}(A)$ from the straight line given by ε_{cur} and ε_0 (cf. fig. 4) we could extract the next two coefficients ε_{-1} and ε_{-2}. However, the accuracy of these coefficients would be much smaller than that of ε_{cur} and ε_0.

4. Remarks on the Strutinsky energy averaging method

The energy averaging method of Strutinsky [2]) has been discussed extensively in the literature [3-7]). We recall here therefore only the main points and then discuss in detail the stationarity condition for the averaged single-particle energy [6]), since it plays an important role in the present considerations.

The smooth, average part of the sum of occupied single-particle energies $\sum_\nu e_\nu$ of one kind of particle is defined by

$$\tilde{U} = \int_{-\infty}^{\lambda} E\tilde{g}(E)\mathrm{d}E, \tag{4.1}$$

where $\tilde{g}(E)$ is the average level density defined by

$$\tilde{g}(E) = \frac{1}{\gamma}\sum_\nu f_{2M}\left(\frac{E-e_\nu}{\gamma}\right). \tag{4.2}$$

The Fermi level is fixed by the equation

$$N = \int_{-\infty}^{\lambda} \tilde{g}(E)\mathrm{d}E. \tag{4.3}$$

In eq. (4.2), $f_{2M}(x)$ is a smooth distribution function (usually a Gaussian) containing the so-called curvature correction of order $2M$. The purpose of this correction is to guarantee that the smooth part $g_0(E)$ of the exact level density,

$$g(E) = \sum_\nu \delta(E-e_\nu), \tag{4.4}$$

is approximated as closely as possible by the quantity $\tilde{g}(E)$, eq. (4.2). In fact, if the smooth part $g_0(E)$, which is dependent on the spectrum e_ν (and thus on the potential used) and may be determined by other methods [13-16,24]), is a polynomial of order $2M+1$ in E, then it is exactly reproduced by $\tilde{g}(E)$. If $g_0(E)$ is any analytical function, then $\tilde{g}(E)$ approximates it by the first $2M+1$ terms of its Taylor expansion around E. The remaining error may be minimized by imposing on the energy $\tilde{U}$, eq. (4.1), the stationarity condition

$$\left.\frac{\partial\tilde{U}}{\partial\gamma}\right|_{\gamma=\gamma_0} = 0, \tag{4.5}$$

as discussed in ref. [6]). Eq. (4.5) is, in fact, the differential form of the usual plateau condition [2]) requiring that the energy $\tilde{U}$ does not depend on the averaging width γ in a region

$$\hbar\omega \lesssim \gamma \ll \lambda. \tag{4.6}$$

The lower limit of γ is the distance between the major shells in the spectrum e_ν. The upper limit may be, practically, smaller than the Fermi energy, if a limited set of levels e_ν is used in eq. (4.2). The plateau condition is usually well fulfilled for Nilsson type potentials. (For the harmonic oscillator potential, it is trivially fulfilled since there $g_0(E)$ is a pure polynomial in E; see e.g. ref. [6]).) In potentials with steeper walls, as e.g. in the Woods-Saxon potential considered in this paper, one has to make use of the stationarity condition (4.5) with the requirement that its solution γ_0 is between the limits given in eq. (4.6). The order $2M$ of the curvature correction has

to be larger than zero: without curvature correction, i.e. for $2M = 0$, the Strutinsky averaging would be equivalent to the temperature smoothing which brings some excitation into the system (cf. e.g. ref. [28])), and eq. (4.5) could not be fulfilled. On the other hand, $2M$ should not be too large, since in the limit $2M \to \infty$, the level density $\tilde{g}(E)$ approaches the exact function $g(E)$, eq. (4.4), independently of the value of γ.

As mentioned already in the introduction, a special problem arises in using finite-depth potentials when the separation energy is comparable with the major shell spacing $\hbar\omega$. In this case, according to eq. (4.6), the Strutinsky averaged energy $\tilde{U}$ depends somewhat on the continuum region, since no levels exist there. Ideally, one should include an analytical continuation of the average level density into the continuum. In practice, however, this is not easy to do. In most practical calculations, one has used [4,5]) some artificial unbound states which are obtained by diagonalizing the one-body Hamiltonian in a harmonic oscillator basis. As demonstrated in ref. [29]), these states lie approximately at the positions of the resonances in the region $0 < E \lesssim 20$ MeV for the usual size of the basis used. Therefore, they might be considered as some approximation to the hypothetical levels of a given nucleus, obtained by extrapolation of real levels of larger nuclei.

In this paper, the energy averaging calculations are performed for the spherical Woods-Saxon potential, for nuclei with mass numbers $A = 40$–600. As mentioned already in sect. 2, the potential has no spin-orbit term and is the same for neutrons and for protons (no Coulomb interaction). Thus, $A = 2N$, where N is the neutron or the proton number. The levels e_ν are obtained by matrix diagonalization in the same way as used and described in refs. [4,7]). The size of the basis is varied to include between 10 shells (in light nuclei) and 14 shells (in heavy nuclei). The unbound levels

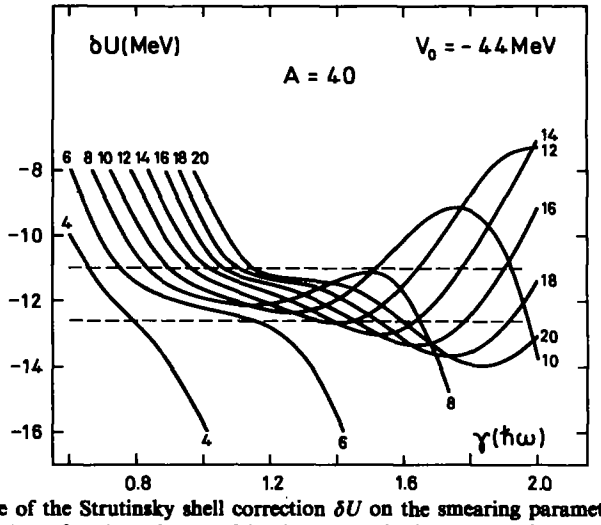

Fig. 5. Dependence of the Strutinsky shell correction δU on the smearing parameter γ, obtained with correcting polynomials of various degrees. The degree $2M$ is shown at each curve. An estimate of an inaccuracy in δU is marked by the dashed lines.

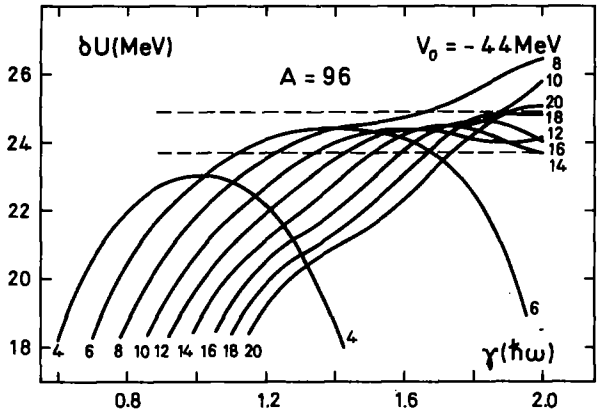

Fig. 6. Same as fig. 5 for the mass number $A = 96$.

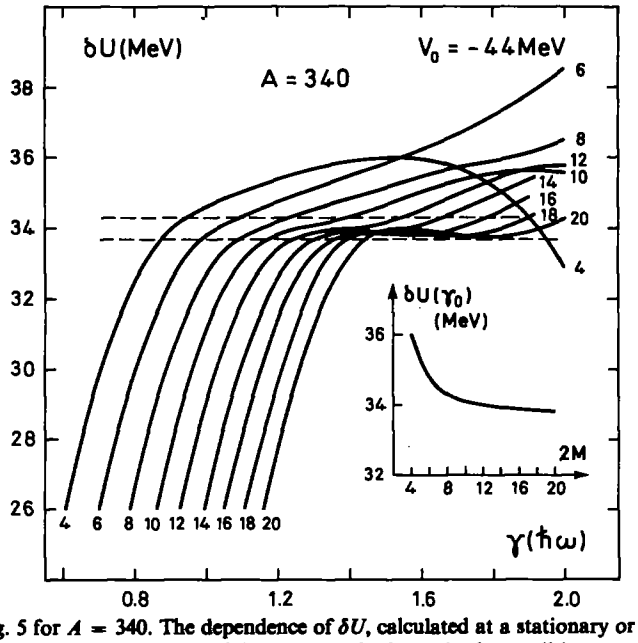

Fig. 7. Same as fig. 5 for $A = 340$. The dependence of δU, calculated at a stationary or deflection point γ_0, on the correcting polynomial degree $2M$ is shown in the small inner graph.

are included up to +30 MeV in light and medium nuclei ($A \lesssim 140$), +20 MeV in heavy ($140 < A \lesssim 360$) and +15 MeV in very heavy nuclei ($360 < A \lesssim 600$), to ensure the numerical convergence of the average energy $\bar{U}$. The stationarity condition is carefully studied in all cases by variation of the smearing parameter γ inside the interval $0.6 \leqq \gamma/\hbar\omega \leqq 2.0$, where

$$\hbar\omega = 41\, A^{-\frac{1}{3}}\ \text{MeV},$$

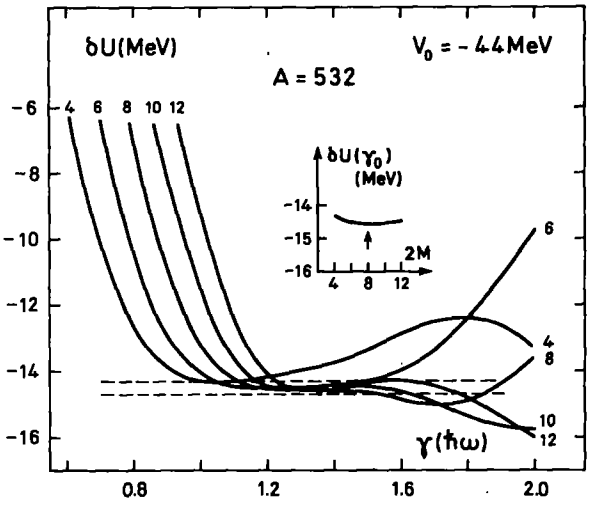

Fig. 8. Same as fig. 7 for $A = 532$.

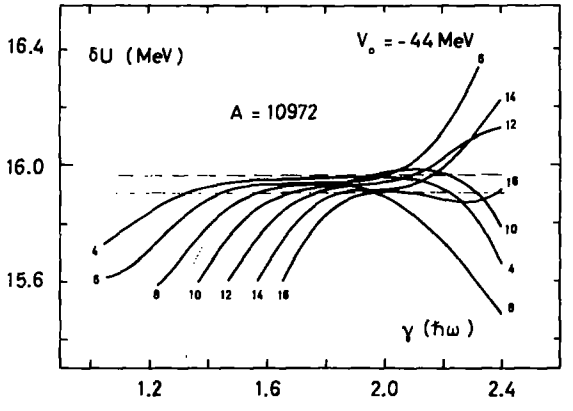

Fig. 9. Same as fig. 5 for a very heavy nucleus, $A = 10972$, when only the bound levels are used to get the plateau.

and by variation of the curvature-correction order $2M$ inside the interval $4 \leqq 2M \leqq 20$.

The results of the study are illustrated in figs. 5–9. To deal with a small quantity, the shell correction

$$\delta U = \sum_{\nu} e_{\nu} - \tilde{U}, \tag{4.7}$$

instead of the energy $\tilde{U}$ itself, is plotted in the figures. As $\sum_{\nu} e_{\nu}$ is independent of the smoothing parameters γ and M, a study of the dependence of $\tilde{U}$ on γ and M is equivalent to that of δU.

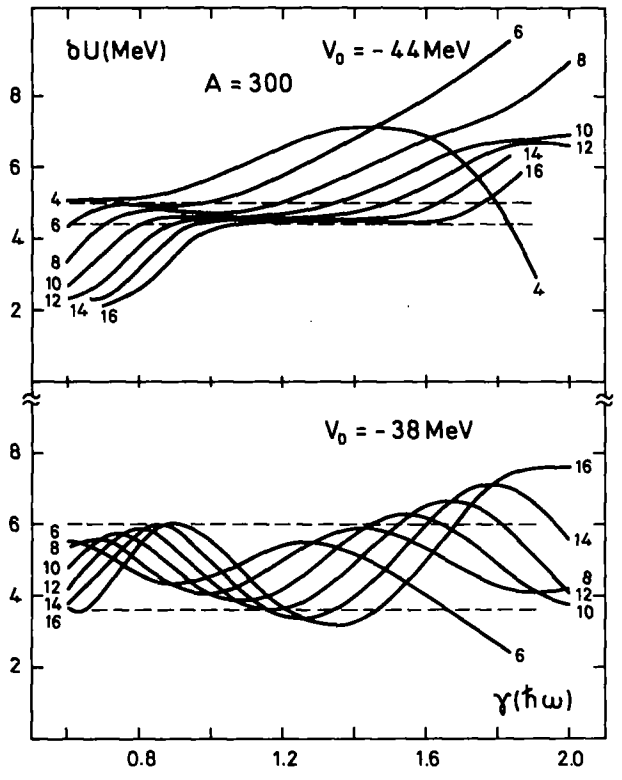

Fig. 10. Comparison between the plateaus obtained with potentials of two different depths.

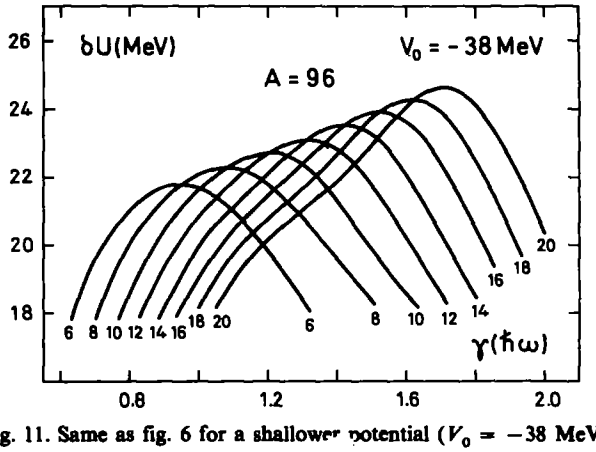

Fig. 11. Same as fig. 6 for a shallower potential ($V_0 = -38$ MeV).

We can see in fig. 5 that for light nuclei, like $A = 40$, the plateau is not very well established either in γ or in M. For small degree of the correction polynomial, like $2M = 6$, there appears only a tendency to form a plateau, marked by a deflection of the δU curve. As a result, the inaccuracy in δU may be established as ± 0.8 MeV (dashed lines in the figure).

For larger A, the plateau improves as can be seen in figs. 6–8. For $A = 340$ (fig. 7), it is already quite well developed in γ (for higher M), but still not in M (cf. the inner plot in the figure). For $A = 532$ (fig. 8), it is already stable in both.

In the asymptotic region, in which we determine the coefficients of the series (2.3), the plateau is extremely well established and is insensitive not only to the unbound but also to the weakly bound levels. Fig. 9 illustrates the plateau for $A = 10972$. We can see (note a fine scale for δU) that δU (i.e. also $\tilde{U}$) is determined with an accuracy of about ± 0.03 MeV. This accuracy is higher, by more than one order, than that for $A = 340$ (fig. 7). For $A \approx 29000$, it is still increased by about one order. This is one of the reasons why we determine ε_{cur} and ε_0 with a rather high accuracy, specified in the previous section, when going to A as large as 30000 in our calculations.

The quality of the plateau is sensitive to the value of the separation energy of a nucleus. This is illustrated in figs. 10 and 11. Fig. 10 shows the effect of about a 4 MeV change in the separation energy (6 MeV change in the potential depth V_0) on the plateau, for the nucleus with $A = 300$. The sensitivity is especially large for light nuclei, where the plateau is rather poor. The decrease of the separation energy by about 4 MeV results in a complete disappearance of the plateau, as can be seen in fig. 11 when compared with fig. 6.

The results of the present section can be summarized as follows:

(i) For realistic mass numbers A (but still not too small, $A \gtrsim 40$) and realistic separation energies, the stationary points of the curves $\delta U(\gamma)$ usually occur within the interval $1.2 \lesssim \gamma_0/\hbar\omega \lesssim 1.8$ and converge as a function of M for $2M \approx 8$–12. The convergence is good for heavy nuclei, but is rather poor for light ones. The stationary values γ_0 and M_0 depend on A.

(ii) The use of fixed values γ_0 and M_0 of the smearing parameters for all A (e.g. $\gamma_0 = 1.2\ \hbar\omega$ and $2M_0 = 6$, as often done, cf. e.g. ref. [3])), instead of finding them for each A separately from the stationarity condition (4.5), may lead to significant differences in δU. This can be seen in figs. 5–8 and will be discussed separately in the next section.

(iii) For heavy nuclei ($A > 120$), an inaccuracy in the plateau value does not usually exceed $\pm(0.7$–$0.8)$ MeV, although there are some local (in A) fluctuations, due to a sensitivity of the plateau to the structure of the spectrum of a given nucleus. For lighter nuclei ($A \lesssim 120$), the inaccuracy may be as large as $\pm(1.2$–$1.5)$ MeV. We think that the inclusion of the spin-orbit splitting will tend to push these numbers slightly down, on the average. Also a deformation of a nucleus, generally tending to make the spectrum more uniform, pushes these numbers down.

In addition to the above, the dependence of the results on the basis dimension N_d

(the number of major oscillator shells) has also been studied. It is found that the plateau is well converged in N_d already at $N_d = 14$, for mass numbers up to $A \approx 350$. For $A \gtrsim 350$ (and up to $A \approx 600$, i.e. up to A for which the energy averaging is studied in the present paper), there still might be a truncation error in δU of around 0.5–1.0 MeV.

5. Discussion

In this section, we would like to make comparisons between different smooth parts $\tilde{U}$ of the total single-particle energy. One comparison is between the asymptotic energy $\tilde{U}_{as}$, eq. (2.3), and the Strutinsky energy, eq. (4.1). The other is between the Strutinsky energies obtained in two slightly different ways. The first way (usually used) is when fixed values of the smearing parameters γ and M (usually $\gamma = 1.2\ \hbar\omega$ and $2M = 6$) are taken for all mass numbers A (and deformations, if the deformation dependence is considered). The second way (optimized) is when both parameters γ and M are varied for each A to get $\tilde{U}$ stationary with respect to both of them. Let us denote the corresponding energies by $\tilde{U}_{Str}$ and $\tilde{U}^{opt}_{Str}$ (and the shell corrections by δU_{Str} and δU^{opt}_{Str}), respectively.

For the asymptotic energy $\tilde{U}_{as}$, we take here the first four terms in the series (2.3), i.e. one or even two terms more than taken usually for the description of the smooth part of the binding energy (droplet or liquid-drop models).

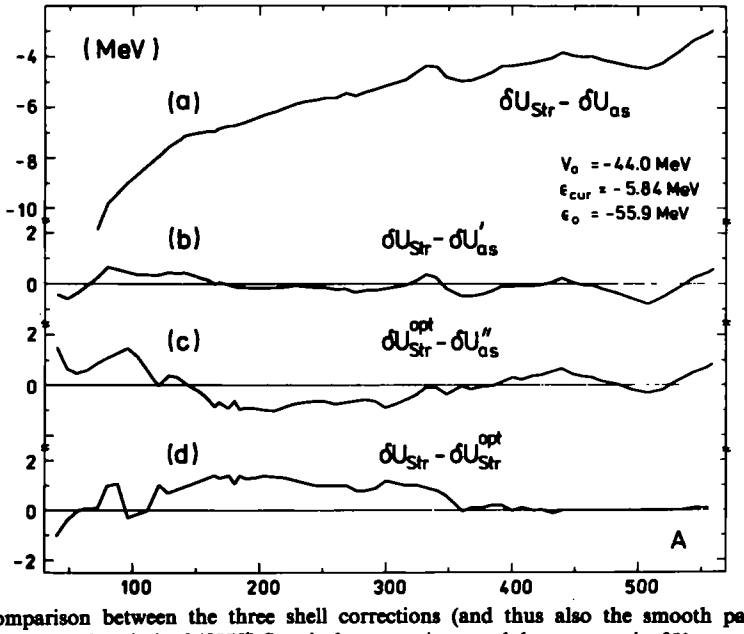

Fig. 12. Comparison between the three shell corrections (and thus also the smooth parts $\tilde{U}$): the usual (δU_{Str}) and optimized (δU^{opt}_{Str}) Strutinsky corrections, and the asymptotic, δU_{as}, correction.

To reduce the scale of the quantities to be compared, we may take the shell corrections δU, eq. (4.7), instead of the energies $\tilde{U}$, as they differ by the quantity $\sum_\nu e_\nu$ which is, in principle, the same in all compared cases. In the case of $\delta U_{\rm Str}$ and $\delta U^{\rm opt}_{\rm Str}$, the sum $\sum_\nu e_\nu$ is exactly the same in both quantities and the comparison between $\delta U_{\rm Str}$ and $\delta U^{\rm opt}_{\rm Str}$ is exactly equivalent to the comparison between $\tilde{U}_{\rm Str}$ and $\tilde{U}^{\rm opt}_{\rm Str}$. In the case of $\delta U_{\rm Str}$ and $\delta U_{\rm as}$, the sum $\sum_\nu e_\nu$ is calculated differently, by diagonalization of the single-particle Hamiltonian in the oscillator basis in the case of $\delta U_{\rm Str}$ and by solution of the Schrödinger equation in the case of $\delta U_{\rm as}$, and thus it differs slightly (and smoothly in A) in the two quantities. Therefore the comparison between $\delta U_{\rm Str}$ and $\delta U_{\rm as}$ is even better than between the smooth parts $\tilde{U}_{\rm Str}$ and $\tilde{U}_{\rm as}$ as the effect of the small differences in e_ν almost disappears when the difference $\sum_\nu e_\nu - \tilde{U}$ is taken.

The results are shown in fig. 12 for the potential with the depth $V_0 = -44$ MeV and in fig. 13 for the shallower potential ($V_0 = -38$ MeV). We can see in fig. 12a that the difference $\delta U_{\rm Str} - \delta U_{\rm as}$ still contains a smooth component, slowly changing with A. This is probably mainly due to the fact that in our asymptotic smooth part $\tilde{U}_{\rm as}$ only the four lowest terms, $\varepsilon_{\rm vol}A$ to ε_0, are taken. As we consider the terms higher than ε_0 unimportant, at least for most applications of the shell correction, let us try to transform off this smooth component from the plot. Assuming it in the form of

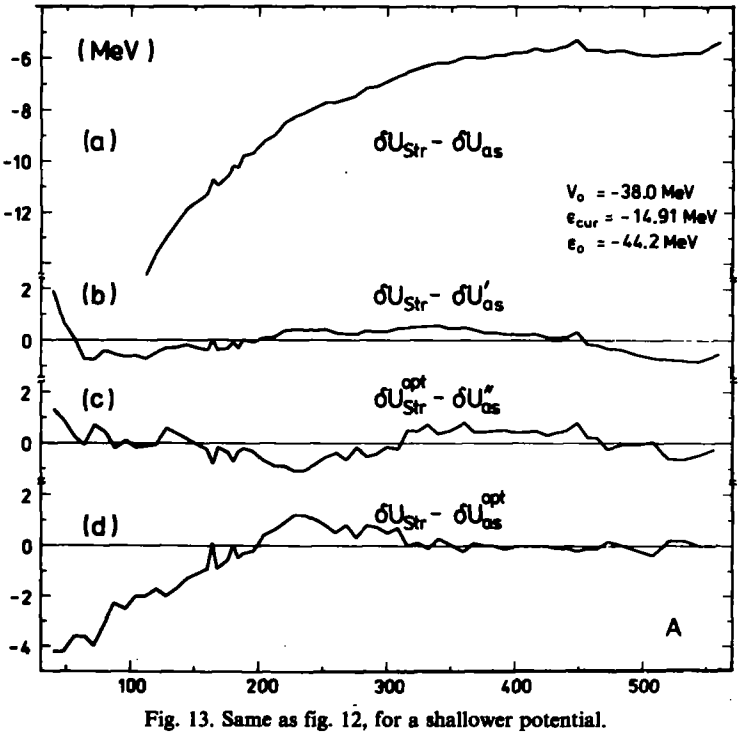

Fig. 13. Same as fig. 12, for a shallower potential.

$-\tilde{\varepsilon}_{-1}A^{-\frac{1}{3}}-\tilde{\varepsilon}_{-2}A^{-\frac{2}{3}}$, we can do this, e.g., by taking

$$\delta U'_{\rm ss} = \delta U_{\rm ss}-\tilde{\varepsilon}_{-1}A^{-\frac{1}{3}}-\tilde{\varepsilon}_{-2}A^{-\frac{2}{3}} \tag{5.1}$$

instead of $\delta U_{\rm ss}$. The coefficients $\tilde{\varepsilon}_{-1}$ and $\tilde{\varepsilon}_{-2}$, calculated so as to minimize the difference $\delta U_{\rm Str}-\delta U'_{\rm ss}$, are obtained as 11.9 and 142 MeV, respectively.

We can see in fig. 12b that $\delta U_{\rm Str}-\delta U'_{\rm ss}$ fluctuates inside limits of about ± 0.7 MeV for lighter nuclei ($A \lesssim 150$) and inside smaller limits for heavier nuclei, giving the accuracy of $\delta U_{\rm Str}$. (The wide dip for $A \approx 500$ and smaller fluctuations for $A \approx 350$ in the curves of figs. 12b and 12c are ascribed by us to the truncation error in our $\tilde{U}_{\rm Str}$ and $\tilde{U}^{\rm opt}_{\rm Str}$ calculations for these heavy nuclei, as mentioned in sect. 4.)

In an identical way, fig. 12c gives the accuracy of $\delta U^{\rm opt}_{\rm Str}$. We can see that the accuracy of $\delta U^{\rm opt}_{\rm Str}$ is smaller than that of $\delta U_{\rm Str}$. Here, the shell correction $\delta U''_{\rm ss}$ is again of the form of (5.1) but with the coefficients $\tilde{\varepsilon}_{-1}$ and $\tilde{\varepsilon}_{-2}$ calculated so as to minimize $\delta U^{\rm opt}_{\rm Str}-\delta U''_{\rm ss}$.

A direct comparison between $\delta U_{\rm Str}$ and $\delta U^{\rm opt}_{\rm Str}$ is given in fig. 12d. It is seen that the difference between the two is inside the limits of about -1.0 to 1.5 MeV, i.e. it is rather large. The usual correction $\delta U_{\rm Str}$ ($\gamma = 1.2\,\hbar\omega$, $2M = 6$) shows a tendency to be too high ("too positive"), by about 1.0–1.5 MeV, for medium and heavy nuclei and too low ("too negative") for light nuclei, with respect to the optimized value $\delta U^{\rm opt}_{\rm Str}$.

Fig. 13 is made in the same way as fig. 12 but for a shallower ($V_0 = -38$ MeV) potential. We can see that for heavy nuclei ($A > 150$), for which the potential gives the separation energies about right, the inaccuracy of $\delta U_{\rm Str}$ is about ± 0.5 MeV and that of $\delta U^{\rm opt}_{\rm Str}$ is about ± 0.8 MeV. Similarly as for the deeper potential, $V_0 = -44$ MeV, the difference $\delta U_{\rm Str}-\delta U'_{\rm ss}$ is more smooth in A than the difference $\delta U^{\rm opt}_{\rm Str}-\delta U''_{\rm ss}$, which means that the energy $\tilde{U}_{\rm Str}$ is more smooth in A than $\tilde{U}^{\rm opt}_{\rm Str}$. Thus, $\delta U_{\rm Str}$ seems better, leading to more accurate results for calculations of the mass differences between neighbouring nuclei (and of the fission barriers, we think) than $\delta U^{\rm opt}_{\rm Str}$.

A direct comparison between $\delta U_{\rm Str}$ and $\delta U^{\rm opt}_{\rm Str}$, fig. 13d, shows an even larger discrepancy than for the $V_0 = -44$ MeV case.

6. Conclusions

The following conclusions may be drawn from our investigation:

(i) For a realistic finite-depth potential, the coefficients of the asymptotic series, eq. (2.3), do not constitute as fastly a decreasing sequence as they do for the infinite harmonic-oscillator potential, eq. (2.4). For this reason, the series seems to converge slowly, especially for mass numbers A that are not too large. However, for most applications of the shell correction obtained with the help of the series, the first three terms seem sufficient.

(ii) The asymptotic energy $\tilde{U}_{\rm ss}$, eq. (2.3), is explicitly a smooth function of A. There is no direct reason, however, for the Strutinsky average energy $\tilde{U}$, eq. (4.1), to be smooth in A. A comparison between the two shows that the Strutinsky energy

has a small component oscillating with A. Its amplitude is about 0.7–0.8 MeV and may be considered as an estimate for the inaccuracy of the Strutinsky average energy $\tilde{U}$, and thus also for the shell correction δU – at least for most applications of δU consisting in a calculation of the mass differences between neighbouring nuclei (e.g. β- and α-decays) or even between the same nucleus but with different deformations (e.g. fission barrier). This estimate is slightly larger than the estimates obtained by other methods [cf. e.g. refs. [5,6]) and references given therein]. However, one should point out that the value 0.7–0.8 MeV for the amplitude is obtained in our case of a large degeneracy of the single-particle levels (no spin-orbit interaction, spherical shape). Inclusion of the spin-orbit splitting and also of the deformation of a nucleus is expected to push this value slightly down.

(iii) The two Strutinsky shell corrections δU_{Str} and $\delta U_{\mathrm{Str}}^{\mathrm{opt}}$ and thus also the average energies $\tilde{U}_{\mathrm{Str}}$ and $\tilde{U}_{\mathrm{Str}}^{\mathrm{opt}}$ (cf. sect. 5), used in the literature, differ somewhat. In our case of a large degeneracy of the single-particle levels, they differ by up to about ± 1.0 MeV, which is of the order of the inaccuracy of these quantities stated above (point (ii)). The energy $\tilde{U}_{\mathrm{Str}}$ is a more smooth function of A than the energy $\tilde{U}_{\mathrm{Str}}^{\mathrm{opt}}$.

(iv) The optimized energy $\tilde{U}_{\mathrm{Str}}^{\mathrm{opt}}$ is more correct than the energy $\tilde{U}_{\mathrm{Str}}$. Still, when calculating the differences between the masses of neighbouring nuclei, it seems better to use the last one. This is just because it is more smooth in A than $\tilde{U}_{\mathrm{Str}}^{\mathrm{opt}}$. The less smooth character of $\tilde{U}_{\mathrm{Str}}^{\mathrm{opt}}$ comes from the fact that for each A we make an independent error when determining the plateau value $\tilde{U}_{\mathrm{Str}}^{\mathrm{opt}}$. Due to this, the errors may sum up when the difference between the masses of arbitrary, even very close in A, nuclei is calculated.

We think that the best procedure, especially when calculating masses of a large number of nuclei, like a mass table, would be the following (cf. also ref. [6])): We find the stationary values $\gamma_0(A)$ and $2M_0(A)$ of the smearing parameters γ and $2M$ for all (or a large enough number of) points A. Then, we determine smooth functions $\tilde{\gamma}_0(A)$ and $2\tilde{M}_0(A)$ (the last is, naturally, a step function), by a best fit to $\gamma_0(A)$ and $2M_0(A)$, and use them for the calculation of the masses.

We would like to thank Professors A. Bohr and B. R. Mottelson for suggesting this problem, for very helpful discussions and their continuous interest in the research. We would also like to thank Drs. J. Dudek, I. Hamamoto, A. S. Jensen, I. Ragnarsson and P. J. Siemens for very useful discussions. Helpful comments by Professors V. M. Strutinsky and W. J. Świątecki are gratefully acknowledged. Two of the authors (M.B. and A.S.) would like to thank the Niels Bohr Institute for the warm hospitality extended to them and the excellent working conditions. One of them (M.B.) gratefully acknowledges the support of the Japan World Exposition Commemorative Fund.

References

1) W. D. Myers and W. J. Swiatecki, Nucl. Phys. **81** (1966) 1
2) V. M. Strutinsky, Sov. J. Nucl. Phys. **3** (1966) 449; Nucl. Phys. **A95** (1967) 420; **A122** (1968) 1
3) S. G. Nilsson, C. F. Tsang, A. Sobiczewski, Z. Szymański, S. Wycech, C. Gustafson, I.-L. Lamm, P. Möller and B. Nilsson, Nucl. Phys. **A131** (1969) 1
4) M. Brack, J. Damgaard, A. S. Jensen, H. C. Pauli, V. M. Strutinsky and C. Y. Wong, Rev. Mod. Phys. **44** (1972) 320
5) M. Bolsterli, E. O. Fiset, J. R. Nix and J. L. Norton, Phys. Rev. **C5** (1972) 1050
6) M. Brack and H. C. Pauli, Nucl. Phys. **A207** (1973) 401
7) H. C. Pauli, Phys. Reports **7C** (1973) 35
8) G. G. Bunatian, V. M. Kolomietz and V. M. Strutinsky, Nucl. Phys. **A188** (1972) 225
9) C. K. Ross and R. K. Bhaduri, Nucl. Phys. **A188** (1972) 566
10) V. M. Strutinsky and F. A. Ivanjuk, Nucl. Phys. **A255** (1975) 405
11) M. Gaudin and A. M. Sajot, Proc. 2nd IAEA Symp. on physics and chemistry of fission (IAEA, Vienna, 1969) p. 229
12) A. S. Tyapin, Sov. J. Nucl. Phys. **11** (1970) 53; **14** (1972) 50
13) R. Balian and C. Bloch, Ann. of Phys. **60** (1970) 401; **64** (1971) 271; **69** (1972) 76
14) R. K. Bhaduri and C. K. Ross, Phys. Rev. Lett. **27** (1971) 606
15) B. K. Jennings, Nucl. Phys. **A207** (1973) 538; Ph.D. thesis, McMaster Univ. (1976)
16) B. K. Jennings, R. K. Bhaduri and M. Brack, Phys. Rev. Lett. **34** (1975) 228; Nucl. Phys. **A253** (1975) 29
17) E. Feenberg, Phys. Rev. **60** (1941) 204
18) W. J. Swiatecki, Proc. Phys. Soc. **A64** (1951) 226
19) D. L. Hill and J. A. Wheeler, Phys. Rev. **89** (1953) 1102
20) E. Hilf and G. Süssmann, Phys. Lett. **21** (1966) 654
21) S. Knaak, G. Süssmann, E. Hilf and H. Büttner, Phys. Lett. **23** (1966) 711
22) W. D. Myers and W. J. Swiatecki, Ann. of Phys. **55** (1969) 395; **84** (1974) 186
23) C. F. Tsang, Ph.D. thesis, report UCRL-18899 (1969);
W. D. Myers, C. F. Tsang and W. J. Swiatecki, notes used by W. J. Swiatecki in his talk given at the Niels Bohr Institute, Copenhagen, 1970 (unpublished)
24) A. Bohr and B. R. Mottelson, Nuclear structure, vol. 2 (Benjamin, Reading, Mass., 1975) ch. 6
25) A. Sugiyama and T. Inoue, J. Phys. Soc. Japan **17** (1962) 759
26) P. J. Siemens and A. Sobiczewski, Phys. Lett. **41B** (1972) 16
27) V. M. Strutinsky, Proc. 7th Masurian School on nuclear physics, 1974, Mikolajki, Poland, Nukleonika **20** (1975) 679
28) M. Brack, Proc. Int. Summer School on nuclear physics, Predeal, Roumania, 1974
29) M. Brack and P. Quentin, Physica Scripta **10A** (1974) 163